

R.M. Yerojwar¹, N.S. Kokode², C.M. Nandanwar², D.K. Ingole¹, R.S. Meshram²

Synthesis and photoluminescence properties of $\text{CaMgAl}_{10}\text{O}_{17}:\text{Sm}^{3+}$ phosphor for n-UV solid-state lighting

¹Department of physics, Mohasinbhai Zaweri Mahavidyalaya, Desaijanj(Wadsa), Gondwana University, Gadchiroli, Maharashtra, India, diptiingole25@gmail.com

²Department of Physics, Nevjabai Hitkarini Mahavidyalaya, Bramhapuri, Gondwana University, Gadchiroli, Maharashtra, India

The combustion method was used to synthesize $\text{CaMgAl}_{10}\text{O}_{17}:\text{Sm}^{3+}$ phosphor. The scanning electron microscopy and photoluminescence properties of phosphors were thoroughly investigated. The emission spectrum has three distinct peaks at 563, 604 and 642 nm under 405 nm excitation, which is corresponding to the transitions $^4\text{G}_{5/2} \rightarrow ^6\text{H}_{5/2}$, $^4\text{G}_{5/2} \rightarrow ^6\text{H}_{7/2}$ and $^4\text{G}_{5/2} \rightarrow ^6\text{H}_{9/2}$ of Sm^{3+} ions. The optimum concentration of $\text{CaMgAl}_{10}\text{O}_{17}:\text{Sm}^{3+}$ phosphor was discovered to be 1 mole %, above which concentration quenching was observed. The CIE coordinates for the $\text{CaMgAl}_{10}\text{O}_{17}$ phosphor with Sm^{3+} ion doped are 604 nm ($x = 0.644$, $y = 0.355$) falling in the red region. According to the current findings, $\text{CaMgAl}_{10}\text{O}_{17}:\text{Sm}^{3+}$ phosphors might be useful in the fields of near UV-excited solid-state lighting.

Keywords: SEM, Photoluminescence, Combustion method, phosphor, solid state lighting, CIE-Coordinates.

Received 30 August 2023; Accepted 20 February 2024.

Introduction

Rare earth ions have been doped in a variety of host materials extensively explored in recent decades due to their distinctive luminescence features. Dy^{3+} , Pr^{3+} , Tb^{3+} , Eu^{3+} and Sm^{3+} ions are significant ion activators for the production of visible light [1-4]. Among these elements, europium and samarium ions can be used as red emitters. Eu^{3+} , Sm^{3+} - activated phosphors like, phosphates, aluminates and silicates for photoluminescence properties are being studied and used for solid state lighting, display [5], optical thermometer applications [6, 7], photocatalysis [8], fingerprint detection and anti-counterfeiting [9].

There have been relatively few contributions to the doping of CaAlO phosphor lattices with Pr^{3+} , Er^{3+} and Eu^{3+} ions in the last several years, but the authors have not highlighted much study on the doping of Sm^{3+} ions in CaAlO phosphor via combustion method. As a dopant, Eu^{3+} ion is often excellent for red phosphor emission [10, 11]. However, the exorbitant expense makes it tough to consider. Sm^{3+} ions are an alternative source of reddish-orange emissions that are much cheaper than Eu^{3+} ions.

When stimulated in near-ultraviolet (n-UV) or blue light, Sm^{3+} ions release reddish-orange light. In addition, trivalent samarium (Sm^{3+}) will exhibit a significant quantum efficiency emission variable as a result of the $^4\text{G}_{5/2} \rightarrow ^4\text{H}_{7/2}$ emitting stage [12]. Overall, the combination of Sm^{3+} ion activators with broad band gap compounds has the potential to be beneficial for optical applications [13]. In this study, Sm^{3+} ion doped $\text{CaMgAl}_{10}\text{O}_{17}$ phosphor powders are synthesized using a combustion process and their photoluminescence, morphological and CIE properties were thoroughly investigated. The produced powders are subjected to a variety of characterization procedures in order to determine their suitability for n-UV solid-state lighting applications.

I. Experimental

The samples of $\text{CaMgAl}_{10}\text{O}_{17}:\text{Sm}^{3+}$ phosphor were prepared by combustion method. Firstly, stoichiometric quantity of source materials $\text{Ca}(\text{NO}_3)_2 \cdot 4\text{H}_2\text{O}$ (A.R.), $\text{Mg}(\text{NO}_3)_2 \cdot 4\text{H}_2\text{O}$ and $\text{Al}(\text{NO}_3)_3 \cdot 9\text{H}_2\text{O}$ (A.R.) and urea (A.R.) for respective molecular formulae of above

mentioned phosphors were taken. Then Sm_2O_3 (A.R.) [as per the impurity added] was dissolved in dilute HNO_3 to convert into $\text{Sm}(\text{NO}_3)_3$. The mixture was introduced into muffle furnace which was maintained at 550°C . Then these samples were reheated at 650°C for 3 hrs and were allowed to cool to reach at room temperature. Finally by crushing sample into a fine powder, it is taken into consideration for the characterization at room temperature.

II. Results and Discussion

2.1. SEM studies

An examination of the surface morphology, $\text{Ca}_2\text{Mg}_2\text{Al}_{28}\text{O}_{46}$ phosphor was investigated using SEM. Figs. 1. (a), (b) and (c), show images with different magnification. The SEM pictures indicate that the lengths are ranging from 5 to 10 micrometer. The crystals have an irregular shape and there is a tendency for plate development with considerable curvature. The micrographs further show this is what crystallites compact, share the boundary with numerous microscopic crystallites [14].

2.2. Photoluminescence study

2.2.1. Photoluminescence properties of

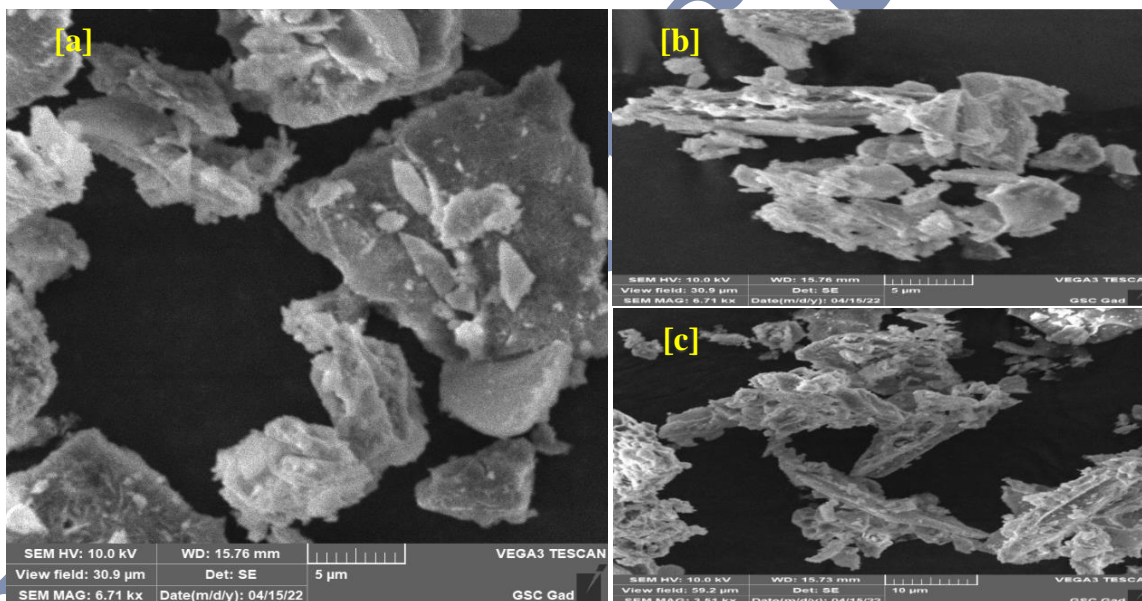


Fig. 1. SEM images of $\text{CaMgAl}_{10}\text{O}_{17}$ phosphor at different magnification.

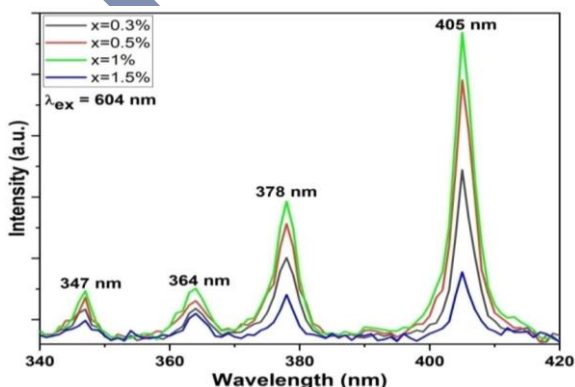


Fig. 2. Spectra of excitation of $\text{CaMgAl}_{10}\text{O}_{17}:\text{Sm}^{3+}$ phosphor monitored at 604 nm emission.

$\text{CaMgAl}_{10}\text{O}_{17}:\text{Sm}^{3+}$ phosphor

As shown in Fig. 2, the excitation curve of the produced $\text{CaMgAl}_{10}\text{O}_{17}:\text{Sm}^{3+}$ phosphors powder were recorded between 340 and 420 nm wavelengths under an emission wavelength of 604 nm. The PL spectrum shows four strong peaks at 347, 364, 378, and 405 nm, this corresponding to ${}^6\text{H}_{5/2}\rightarrow{}^4\text{H}_{9/2}$, ${}^6\text{H}_{5/2}\rightarrow{}^4\text{D}_{3/2}$, ${}^6\text{H}_{5/2}\rightarrow{}^4\text{D}_{1/2}$ and ${}^6\text{H}_{5/2}\rightarrow{}^4\text{F}_{7/2}$, respective transitions [15]. The picture shows that the PL band centered at 405 nm (${}^6\text{H}_{5/2}\rightarrow{}^4\text{F}_{7/2}$) has the highest when compared with its intensity equivalents, indicating that the ${}^4\text{F}_{7/2}$ level is the most populated and that all manufactured powders are now pushed with a wavelength in the 405 nm range.

The range of PL emission spectrum reported between 525-675 nm by observing for fixed excitation wavelength of 405 nm, as shown in Fig. 3. The emission spectrum has three distinct peaks at 563, 604 and 642 nm. In other words, the corresponding transitions of sm^{3+} ions are ${}^4\text{G}_{5/2}\rightarrow{}^6\text{H}_{5/2}$, ${}^4\text{G}_{5/2}\rightarrow{}^6\text{H}_{7/2}$ and ${}^4\text{G}_{5/2}\rightarrow{}^6\text{H}_{9/2}$ [16, 17]. The process speeds via non-radiative reduction to ${}^4\text{G}_{5/2}$ after stimulation from ground level to excited levels (shown in the energy level diagram). Energy separation between these phases reduces the possibility of additional non-radiative relaxation cascades. As shown in the picture with vertically down arrow heads, excited Sm^{3+} ions undergo radiative decreases to inferior sites ${}^6\text{H}_{5/2}$, ${}^6\text{H}_{7/2}$, and ${}^6\text{H}_{9/2}$.

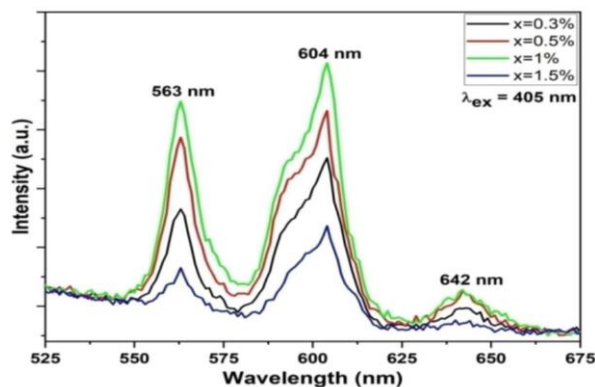


Fig. 3. PL emission spectra of $\text{CaMgAl}_{10}\text{O}_{17}:\text{Sm}^{3+}$ phosphor at excitation 405 nm.

The emission spectrum clearly shows that the transition caused by ${}^4\text{G}_{5/2} \rightarrow {}^6\text{H}_{5/2}$ is because it fulfills the assortment law $J=1$, MD (magnetic dipole) conversion. The transition caused by ${}^4\text{G}_{5/2} \rightarrow {}^6\text{H}_{9/2}$, on the other hand, obeys $J = 2$ assortments rule and is an ED (electric dipole) conversion.

Furthermore, the strongest emission peak, located at 604 nm (${}^4\text{G}_{5/2} \rightarrow {}^6\text{H}_{7/2}$), portrays a primary red emission that follows MD and partly ED acceptable conversion because as it is ED promoting and appears $J = 1$ [18]. After the strength percentage of ED to MD transitions, the configuration of the surrounding environment around the RE 4f ions may generally be investigated. Thus, in present investigation, the MD's transition emission amplitude (${}^4\text{G}_{5/2} \rightarrow {}^6\text{H}_{5/2}$) is found to be bigger than that of the transition ED (${}^4\text{G}_{5/2} \rightarrow {}^6\text{H}_{9/2}$), indicating that the ligand's atmosphere is more consistent [19].

Intensity variation curve for Sm^{3+} ion doping concentration at 604 nm of $\text{CaMgAl}_{10}\text{O}_{17}:\text{Sm}^{3+}$ phosphor shown in Fig. 4. It is discovered that when the proportion of Sm^{3+} ion in the host lattice increases, the strength of the emission peak rises by up to 1 mole %. Following that, the intensity begins to decrease as the Sm^{3+} ion concentration increases. As a consequence, the ideal molar proportion of Sm^{3+} ions doped $\text{CaMgAl}_{10}\text{O}_{17}$ phosphor was determined to be 1 mole %. The concentration quenching effect is responsible for the reduction in emission intensity [20].

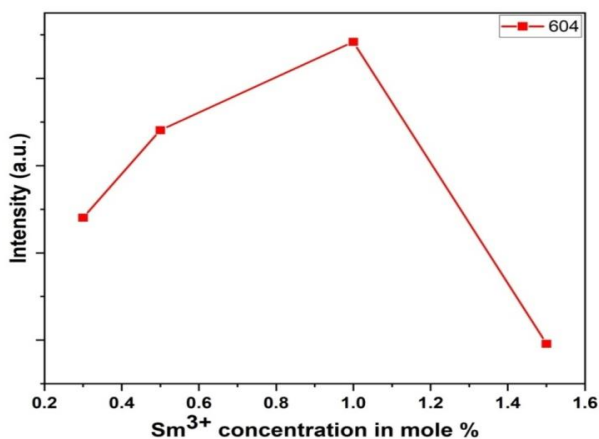


Fig. 4. Intensity variation curves for Sm^{3+} ion doping concentration at 604 nm $\text{CaMgAl}_{10}\text{O}_{17}:\text{Sm}^{3+}$ phosphors.

2.3. Chromaticity

The CIE 1931 (commission international de l'Eclairage) coordinates of microcrystalline powders were analyzed to assess the capabilities of the manufactured microcrystalline powders for application in lighting systems (Fig. 5.). The CIE hue coordinates are calculated using CIE tools to study the color scheme of produced powders [21]. The CIE color coordinates were calculated using the emission spectrum data from all doped samples stimulated at 405 nm, as shown in Fig. 5. All of the color values are discovered to be in the bright orange-red zone. The co-ordinates correspond to 604 nm and 643 nm, with values of (0.644, 0.355) and (0.720, 0.279) for 1 mole %

Sm^{3+} ion doped powder, respectively. The image shows that when the quantity of Sm^{3+} ions increases, the emission spectra show deep red in the color [22]. When combined with other phosphor powders, the color attributes of the produced these phosphors may be employed efficiently in red wavelength emitting devices and as possible phosphor in the production of solid state lighting.

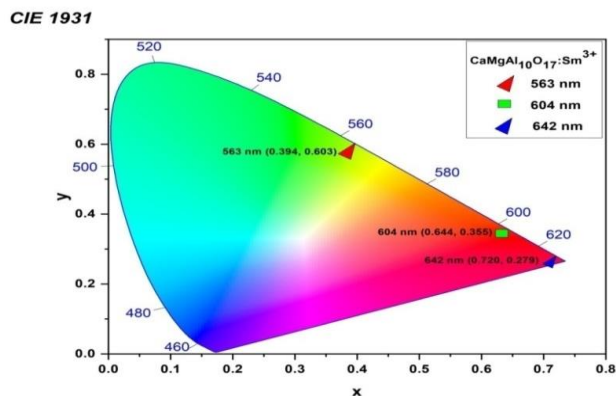


Fig. 5. Diagram showing CIE coordinates $\text{CaMgAl}_{10}\text{O}_{17}:\text{Sm}^{3+}$ phosphor.

Conclusion

The combustion method was used to produce $\text{CaMgAl}_{10}\text{O}_{17}:\text{Sm}^{3+}$ phosphor. Study was also done on morphological and photoluminescence's properties. The $\text{CaMgAl}_{10}\text{O}_{17}:\text{Sm}^{3+}$ phosphors excitation at 405 nm with emission spectrum peaks at 563, 604 and 642 nm. The results show that the optimum $\text{CaMgAl}_{10}\text{O}_{17}:\text{Sm}^{3+}$ phosphor doping amount is 1 mole %. The closest neighbour interaction plays an important role in concentration quenching. Chromaticity generalization results in the coordinates value being the same as for the most intense emission wavelength (0.644, 0.355). According to the photoluminescence results, $\text{CaMgAl}_{10}\text{O}_{17}:\text{Sm}^{3+}$ phosphors might be useful in the fields of near UV-excited solid state lighting.

Declaration of Competing Interest

The authors declare that they do not have any known competing financial interests or personal ties that may seem to have influenced the work reported in this paper.

Data availability

Data will be made available on request.

Yerojwar R.M. – M.Sc. SET, Assistant Professor;
Kokode N.S. – Ph.D, Professor;
Nandanwar C.M. – M.Sc. NET, Research Scholar;
Ingole D.K. – Ph.D, Assistant Professor;
Mesram R.S. – M.Sc. (Physics), Assistant Professor.

[1] S.A.Naidu, S.Boudin, U.V.Varadaraju, B.Raveau, *Eu³⁺ and Tb³⁺ Emission in Molybdenophosphate Na₂Y(MoO₄)(PO₄)*, Journal of the Electrochemical Society, 159, J122 (2012); <https://doi.org/10.1149/2.071204jes>.

- [2] C.M. Nandanwar, N.S. Kokode, *Synthesis and Photoluminescence Properties of $\text{Ca}_5(\text{PO}_4)_3\text{F}:\text{Ln}$ (Ln: Dy^{3+} , Eu^{3+} and Sm^{3+}) Phosphors for near UV-based solid state lighting*, Physics and Chemistry of solid state, 23 (3), 597, (2022); <https://doi.org/10.15330/pcss.23.3.597-603>.
- [3] J.Zhu, J.Xiang, L.Hu, Y.Mao, K.Xiong, H. Zhao, *Synthesis and red emitting properties of $\text{NaAlP}_2\text{O}_7:\text{Pr}^{3+}$ polycrystal for blue chip-excited WLEDs*, Results in Physics, 12, 771, (2019); <https://doi.org/10.1016/j.rinp.2018.12.047>.
- [4] A.N.Yerpude, G.N.Nikhare, S.J.Dhoble, N.S.Kokode, *Luminescence Properties Of Rare Earth Sm^{3+} and Tb^{3+} Doped $\text{Ca}_3\text{Al}_2\text{O}_6$ Phosphor For Solid State Lighting*, Materials Today: Proceedings, 15, 511 (2019); <https://doi.org/10.1016/j.matpr.2019.04.115>.
- [5] A. K. Vishwakarma, M. Jayasimhadri, *Pure orange color emitting Sm^{3+} doped BaNb_2O_6 phosphor for solid-state lighting applications*, J. Lumin. 176, 112, (2016); <https://doi.org/10.1016/j.jlumin.2016.03.025>.
- [6] D. Stefanska, B. Bondzior, T.H.Q. Vu, N. Miniajluk-Gawel, P.J. Deren, *The influence of morphology and Eu^{3+} concentration on luminescence and temperature sensing behavior of Ba_2MgWO_6 double perovskite as a potential optical thermometer*, J. Alloys Compd. 842, 155742, (2020); <https://doi.org/10.1016/j.jallcom.2020.155742>.
- [7] R.M. Yerojwar, N.S. Nandanwar, C.M. Kokode, D.K. Ingole, G.R. Nimbarte, *Combustion Synthesis and Photoluminescence Properties of Novel $\text{Bi}_2\text{Al}_4\text{O}_9:\text{Eu}^{3+}$ Phosphor for n-UV w-LEDs*, Journal of Fluorescence. 33, 1, (2023); <https://doi.org/10.1007/s10895-023-03313-0>.
- [8] D. Wei, J. Bai, Y. Huang, H.J. Seo, *Surface oxygen defects induced via lowtemperature annealing and its promotion to luminescence and photocatalysis of Eu^{3+} -doped $\text{Te}_3\text{Nb}_2\text{O}_{11}$ nanoparticles*, Appl. Surf. Sci. 533, 147502, (2020); <https://doi.org/10.1016/j.apsusc.2020.147502>.
- [9] H. Trabelsi, M. Akl, S.H. Akl, *Ultrasound assisted Eu^{3+} -doped strontium titanate nanophosphors: Labeling agent useful for visualization of latent fingerprints*, Powder Technol. 384, 70, (2021); <https://doi.org/10.1016/j.powtec.2021.02.006>.
- [10] X. Huang, H. Guo, *$\text{LiCa}_3\text{MgV}_3\text{O}_{12}:\text{Sm}^{3+}$: A new high-efficiency white-emitting phosphor*, Ceram. Int. 44, 10340, (2018); <https://doi.org/10.1016/j.ceramint.2018.03.043>.
- [11] X. Huang, S. Wang, B. Li, Q. Sun, H. Guo, *High-brightness and high-color purity red-emitting $\text{Ca}_3\text{Lu}(\text{AlO})_3(\text{BO}_3)_4:\text{Eu}^{3+}$ $\text{Ca}_3\text{Lu}(\text{AlO})_3(\text{BO}_3)_4:\text{Eu}^{3+}$ phosphors with internal quantum efficiency close to unity for near-ultraviolet-based white-light-emitting diodes*, Opt. Lett. 43, 1307, (2018); <https://doi.org/10.1364/OL.43.001307>.
- [12] R.T. Maske, A.N. Yerpude, S.J. Dhoble, *Wet chemical synthesis of Sm^{3+} doped $\text{Ca}_{10}(\text{PO}_4)_6\text{Cl}_2$ phosphor for w-LED application*, Materials Letters: X. 19, 100214, (2023); <https://doi.org/10.1016/j.mlblux.2023.100214>.
- [13] R.B. Basavaraj, H. Nagabhushana, B. Daruka Prasad, S.C. Sharma, S.C. Prashantha, B.M. Nagabhushana, *A single host white light emitting $\text{Zn}_2\text{SiO}_4:\text{Re}^{3+}$ (Eu, Dy, Sm) phosphor for LED applications*, Optik. 126, 1745, (2015); <https://doi.org/10.1016/j.ijleo.2014.07.149>.
- [14] C.M. Nandanwar, N.S. Kokode, A.N. Yerpude, S.J. Dhoble, *Combustion synthesis of $\text{KZnPO}_4:\text{RE}$ (RE = Dy^{3+} and Sm^{3+}) Phosphors for n-UV based w-LEDs*, Eur. Phys. J. Appl. Phys., 98, 50, (2023); <https://doi.org/10.1051/epjap/2023230073>.
- [15] V. Singh, G. Lakshminarayana, A. Wagh, *Sol-gel synthesis and fluorescence features of $\text{SrAl}_4\text{O}_7:\text{Sm}^{3+}$ phosphors*, Optik. 204, 163908 (2019); <https://doi.org/10.1016/j.ijleo.2019.163908>.
- [16] Y.R. Shi, G.W. Ge, L.X. Yang, C.Y. Li, Z. L. Wang, *Structure and photoluminescence properties of $\text{Ca}_2\text{GdZr}_2\text{Al}_3\text{O}_{12}:\text{RE}^{3+}$ (RE $^{3+}$ = Eu, Sm, Pr, Dy, Tb) phosphors*, J. Mater. Sci. Mater. Electron, 29, 771 (2018); <https://doi.org/10.1007/s10854-017-7971-6>.
- [17] C.M. Nandanwar, N.S. Kokode, A.N. Yerpude, S.J. Dhoble, *Luminescence properties of $\text{BiPO}_4:\text{Ln}$ (Ln = Dy^{3+} , Tb^{3+} and Sm^{3+}) orthophosphate phosphors for near-UV-based solid-state lighting*, Bulletin of Materials Science. 46, 51, (2023); <https://doi.org/10.1007/s12034-023-02900-y>.
- [18] Z. Zhang, J. Li, N. Yang, Q. Liang, X. Yiqin, F. Shuting, J. Yan, J. Zhou, J. Shi, M. Wu, *A novel multi-center activated single-component white light-emitting phosphor for deep UV chip-based high color-rendering WLEDs*, Chem. Eng. J. 390, 124601 (2020); <https://doi.org/10.1016/j.cej.2020.124601>.
- [19] K.R. Kalimuthu, S.M. Babu, V. Kalimuthu, *Synthesis and photoluminescence properties of Sm^{3+} doped $\text{LiGd}(\text{WO}_4)_2$ phosphors with high color purit*, Opt. Mater. 102, 109804 (2020).
- [20] Dhoble *Effect of alkali metal ions A^+ (A = K^+ , Na^+ and Li^+) on the photoluminescence properties of $\text{Sr}_3\text{Bi}(\text{PO}_4)_3:\text{Sm}^{3+}$ phosphors prepared by wet chemical synthesis*, Result in Optics. 12, 100456 (2023); <https://doi.org/10.1016/j.rio.2023.100456>.
- [21] S. Kaur, M. Jayasimhadri and A. S. Rao, *A novel red emitting Eu^{3+} doped calcium aluminozincate phosphor for applications in w-LEDs*, J. Alloys Compd. 697, 367 (2017); <https://doi.org/10.1016/j.jallcom.2016.12.150>.
- [22] R.M. Yerojwar, N.S. Kokode, C.M. Nandanwar, D.K. Ingole, S.T. Peddiwar, *Photoluminescence characteristics of novel Sm^{3+} ions-doped $\text{La}_{1.4}\text{Al}_{22.6}\text{O}_{36}$ phosphor for n-UV w-LED*, Luminescence. 38, 1536 (2023); <https://doi.org/10.1002/bio.4533>.

Р.М. Єроджвар, Н.С. Кокоде, К.М. Нанданвар, Д.К. Инголе, Р.С. Мешрам

Синтез і фотолюмінесцентні властивості люмінофора $\text{CaMgAl}_{10}\text{O}_{17}:\text{Sm}^{3+}$ для ближнього УФ-твердотільного освітлення

Кафедра фізики, університет Гондвани, Гадчиролі, Махараїшта, Індія, diptiingole25@gmail.com.

Методом спалювання синтезовано люмінофор $\text{CaMgAl}_{10}\text{O}_{17}:\text{Sm}^{3+}$. Проведено СЕМ-дослідження та дослідження фотолюмінесцентних властивостей люмінофорів. Показано, що спектр випромінювання має три чіткі піки при 563, 604 і 642 нм під час збудження 405 нм, що відповідає переходам ${}^4\text{G}_{5/2} \rightarrow {}^6\text{H}_{5/2}$, ${}^4\text{G}_{5/2} \rightarrow {}^6\text{H}_{7/2}$ і ${}^4\text{G}_{5/2} \rightarrow {}^6\text{H}_{9/2}$ іонів Sm^{3+} . Виявлено, що оптимальна концентрація люмінофора $\text{CaMgAl}_{10}\text{O}_{17}:\text{Sm}^{3+}$ становить 1 мол.%, вище якої спостерігалось концентраційне гасіння. Координати СІЕ для люмінофора $\text{CaMgAl}_{10}\text{O}_{17}$ із додаванням іонів Sm^{3+} становлять 604 нм ($x = 0,644$, $y = 0,355$), що відноситься до червоної області. Згідно з поточними висновками, люмінофори $\text{CaMgAl}_{10}\text{O}_{17}:\text{Sm}^{3+}$ можуть бути корисними для реалізації ближнього УФ-випромінювання у твердотільних пристроях.

Ключові слова: СЕМ, фотолюмінесценція, метод горіння, люмінофор, твердотільне освітлення, СІЕ-координати.

Retracted